

Electronic Supplementary Information (ESI)

Quantum dot/ methylene blue FRET mediated NIR fluorescent nanomicelles with large Stokes shift for bioimaging†

Li Li,‡ Jianbo Liu,‡ Zhihong Peng, Xiaohai Yang, Wei Liu, Jianguo Xu, Jinlu Tang, Xiaoxiao He, Kemin Wang**

State Key Laboratory of Chemo/Biosensing and Chemometrics, College of Biology and Chemical Engineering, Hunan University. Key Laboratory for Bio-Nanotechnology and Molecular Engineering of Hunan Province, Changsha 410082, China.

† L. Li and J.B. Liu contributed equally to this work.

* Email: kmwang@hnu.edu.cn; xiaoxiaohe@hnu.edu.cn .

Experimental Section

1. Materials and Instruments.

Cetyltrimethylammonium bromide (CTAB) and methylene blue (MB) were purchased from Aldrich. Hydrophobic Core/Shell CdSe/ZnS QDs stabilized by octadecylamine were prepared as described previously with minor modification,^{1,2} and the QDs with fluorescence peak at 630 nm were used. Unless otherwise noted, all reagent-grade chemicals were used as received. The water used in all experiments was of Millipore Milli-Q grade. HepG2 cells used in this study were obtained from Cell Bank of the Committee on Type Culture Collection of the Chinese Academy of Sciences (Shanghai, China). UV-vis spectroscopy measurements were conducted using a Shimadzu UV-1601 spectrophotometer in transmission mode and a quartz cuvette (10 mm). The photoluminescence spectra were recorded on a PTI QM40-NIR Fluorescence Lifetime Spectrometers, and the excitation wavelength was set at 488 nm and the emitted fluorescence was collected in the NIR region (680–750 nm). The hydrodynamic sizes and zeta potentials were measured in a Nano-ZS analyzer (Malvern). Transmission electron microscopy (TEM) was performed on a JEOL-1230 microscope. The samples for TEM were obtained by drying sample droplets from water dispersion onto a Cu grid coated with a lacey carbon film, which was then allowed to dry prior to imaging.

2. Fabrication of Quantum Dots/ Methylene Blue Nanomicelles.

The QDs/MB nanomicelles were fabricated through typical surfactant-assisted, evaporation induced microemulsion approach. A concentrated solution of QDs in chloroform was added to an aqueous solution of CTAB and MB under vigorous stirring to create an oil-in-water microemulsion. Chloroform evaporation during a heat course (40–80 °C, ~10 min) transfers the QDs into the aqueous phase (forming QDs/MB nanomicelles stock solution). This interfacial process is driven by the hydrophobic Vander Waals interactions between the primary alkane of the stabilizing ligand and the secondary alkane of the surfactant, resulting in thermodynamically defined, interdigitated bilayer structures (Scheme S1).

In a typical nanomicelles synthesis procedure, CTAB (0.20 g) and MB (0.112 mg) was added to deionized water (10 mL) to form solution A. Solution A was sonicated to completely dissolve the surfactant. Hydrophobic CdSe/ZnS QDs stabilized by octadecylamine (0.10 g) were dissolved in chloroform (2 mL) to form solution B. Solutions A and B were mixed together with vigorous stirring, and the chloroform was removed by heat treatment to finish the encapsulation. A dark red colored solution (stock solution, C) was finally obtained and centrifuged at 50000 rpm for 2 h to remove any precipitates. After purifying, the obtained QDs/MB nanomicelles suspension was dissolved in 10 mL deionized water.

As control experiment, QDs nanomicelles without MB (QDs nanomicelles) were prepared, and MB nanomicelles without QDs (MB nanomicelles) were also prepared.

3. Colloidal stability and photostability of QDs/MB nanomicelles

The colloidal stability of fluorescence nanomicelles is essentially important for their application in vivo small animal imaging.

Firstly, the colloidal stability at different buffer solutions were investigated. PBS, Tris-HCl and HEPES buffer solutions at 10 mM, pH 7.4 were prepared. QDs/MB nanomicelles were dispersed

in PBS, Tris-HCl and HEPES buffers respectively. After stored for 30 min, their photograph and fluorescent imaging could be obtained.

Secondly, the thermal stability of the nanomicelles was studied. QDs/MB nanomicelles were dispersed in Tris-HCl buffer and their hydrodynamic sizes were determined at 20 °C, 40 °C and 60 °C, respectively.

Beside, the fluorescence intensity of QDs/MB nanomicelles in full mouse serum for up to 5 h was also measured. At scheduled intervals, the fluorescence intensity of QDs/MB nanomicelles was obtained by a fluorometer. The initial fluorescence intensity of QDs/MB nanomicelles in the solution signs as F_0 . The fluorescence intensity of QDs/MB nanomicelles at other time was measured as F . The normalized fluorescence intensity variation of QDs/MB nanomicelles was calculated by using the relation $F/F_0 \times 100\%$.

Moreover, The photostability of QDs/MB nanomicelles were also measured by a fluorometer when exposed to UV light for up to 5 h at room temperature. At scheduled intervals, the initial fluorescence intensity of QDs/MB nanomicelles in the solution signs as F_0 . Then, the fluorescence intensity of QDs/MB nanomicelles at other time signs as F . The photostability curve of QDs/MB nanomicelles was plotted by using the normalized fluorescence intensity variation ($F/F_0 \times 100\%$).

4. Cytotoxicity of QDs/MB nanomicelles

The cytotoxicity of QDs/MB nanomicelles was evaluated by an MTT assay using HepG2 cell and. HepG2 cells were seeded onto 96-well plates at a density of 7×10^3 cells per well in 200 μ L of medium containing 10% fetal calf serum and incubated at 37 °C and 5% CO₂. After grown overnight, 200 μ L of new medium containing various concentrations of QDs/MB nanomicelles was added into HepG2 cells. After incubated for 24 h, all cells were further incubated with fresh medium containing MTT (0.5 mg/mL) for 4 h. Then the medium was withdrawn and 150 μ L of DMSO was added into each well to dissolve the precipitated formazan violet crystals at 37 °C for 10 min. The absorbance was measured at 490 nm by a multidetection microplate reader.

5. Living cell NIR imaging

Liver Cancer HepG2 Cell were seeded at a density of 5×10^3 cells in 96-well plates and cultured in RPMI 1640 culture medium with 10 % fetal bovine serum in a humidified incubator with 5 % CO₂ at 37 °C for 24 h. The nanomicelles were added into the cells respectively. The cellular uptake was investigated using fluorescent imaging techniques. Fluorescence imaging was conducted using a confocal laser scanning microscopy setup consisting of a heated specimen holder and an Olympus IX-70 inverted microscope with an Olympus FluoView 500 confocal scanning system. The cellular images were taken with a 40 \times objective. The samples were excited with 488 nm laser and the emitted fluorescence was collected through 660 nm longpass filter.

6. NIR imaging in vivo

Male athymic BALB/c(Balb/C-nu) mice were obtained from the Hunan Slaccas Jingda Laboratory Animal Co., Ltd., (BALB/c). They were 4–5 weeks old at the start of each experiment and weighed 20–25 g. All animal operations were in accord with institutional animal use and care regulations, according to protocol no. SYXK (Xiang) 2008-0001, approved by the Laboratory Animal Center of Hunan. Fluorescence images of live mice were taken by an IVIS Lumina II in vivo imaging system (Caliper Life Science, USA). Before imaging, BALB/c nude mice, were

anesthetized with the combined use of tranquilizer and anesthetic. Fluorescence imaging of the mice was performed after subcutaneous injections of 50 μL QDs/MB nanomicelles, as the same dose QDs nanomicelles and MB nanomicelles for comparison. Time of exposure for every fluorescence image was 200 ms. The background fluorescence imaging of the nude mice and nanomicelles imaging were directly obtained without use of spectral unmixing techniques. All the fluorescence images were presented after processing by Image J software. The nude mice were excited with 488 nm laser and the emitted fluorescence was collected in the NIR region (680–800 nm).

7. Analysis of FRET efficiency

The experimental FRET efficiency E was calculated for each sample, which is obtained by eqn (S1).

$$E = \frac{F_D - F_{DA}}{F_D} \quad (\text{S1})$$

where F_D and F_{DA} are the fluorescence intensities of the donor (QDs) alone and the donor in the presence of acceptor (MB).³

The Förster radius (R_0) for which the energy transfer efficiency is diminished to 50% of the maximal value is calculated using eqn (S2).⁴

$$R_0^6 = 8.96 \times 10^{-5} (\kappa^2 n^{-4} Q_d J) \quad (\text{S2}).$$

where κ is an orientation factor, which is regarded as $2/3$ for a randomly orientated donor–acceptor pair; n is the refractive index of the medium, which is 1.33 for water; Q_d is the quantum yield of the donor in the absence of acceptors and calculated as a procedure reported by the literature,⁵ which is 61% for QDs; J is the spectral integral as a function of wavelength, expressing the spectral overlap between the emission spectrum of the donor and the absorption spectrum of the acceptor, which is obtained by eqn (S3)

$$J = \frac{\int_0^\infty F_D(\lambda) \varepsilon A(\lambda)^4 d\lambda}{\int_0^\infty F_D(\lambda) d\lambda} \quad (\text{S3}).$$

Where $F_D(\lambda)$ is the dimensionless emission intensity; λ is the wavelength; $\varepsilon A(\lambda)$ is the molar absorption coefficient of MB at λ . The calculated overlap integral is around $1.3911 \times 10^{-17} \text{ M}^{-1} \text{ cm}^{-1} \text{ nm}^4$. Thus the Förster radius is calculated to be 10.8 Å according to eqn (S1) with the help of the software Matlab.

The efficiency E of a FRET process can also be calculated using eqn (S4),

$$E = \frac{R_0^6}{R_0^6 - R^6} \quad (\text{S4})$$

8. quantum yield

The PL quantum yield was obtained by referencing to a standard Rhodamine 6G (QY = 95% in

ethanol). The PL quantum yield was calculated using the following equation (S5):

$$\Phi = \Phi_{ST} \left(\frac{\text{Grad}_x}{\text{Grad}_{ST}} \right) \left(\frac{\eta_x^2}{\eta_{ST}^2} \right) \quad (\text{S5})$$

Where the subscripts ST and X denote standard (Here, Rhodamine 6G as standard) and test respectively, Φ is the fluorescence quantum yield, Grad the gradient from the plot of integrated fluorescence intensity vs absorbance, and η the refractive index of the solvent.

QY of QDs used in this experiment was calculated as 61% according above algorithm.

Legend

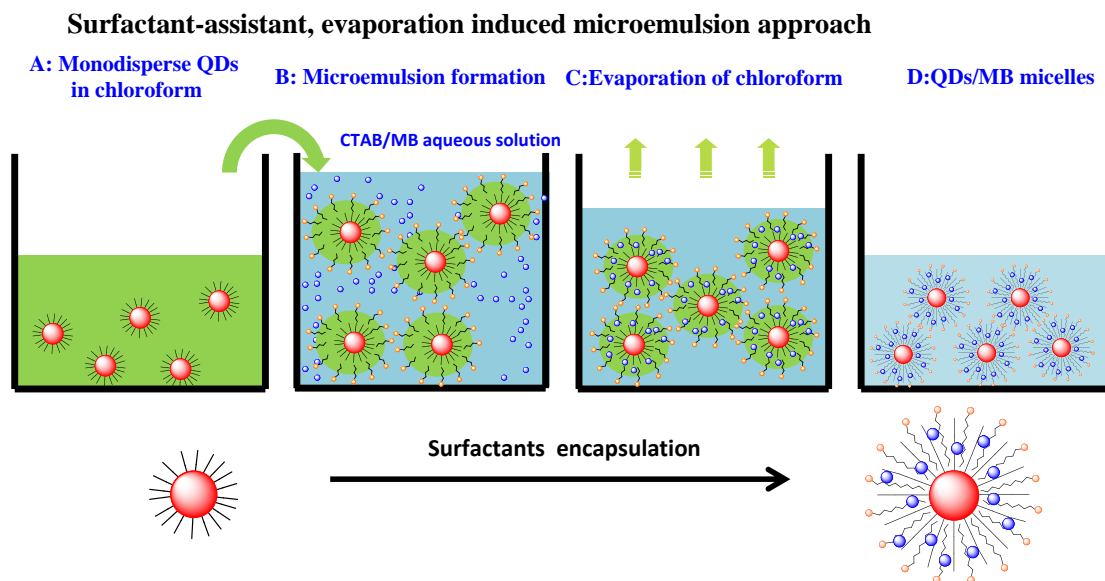


Figure S1. Formation of water-soluble QDs/MB nanomicelles through surfactant encapsulation. (A) Hydrophobic QDs in chloroform solution. (B) Addition chloroform containing of monodisperse hydrophobic QDs into surfactants leads to the formation of a water-in-oil microemulsion. (C) Evaporation of the chloroform transfers the QDs into the aqueous phase to form QDs/MB nanomicelles. (D) Thermodynamically defined interdigitated bilayer structures.

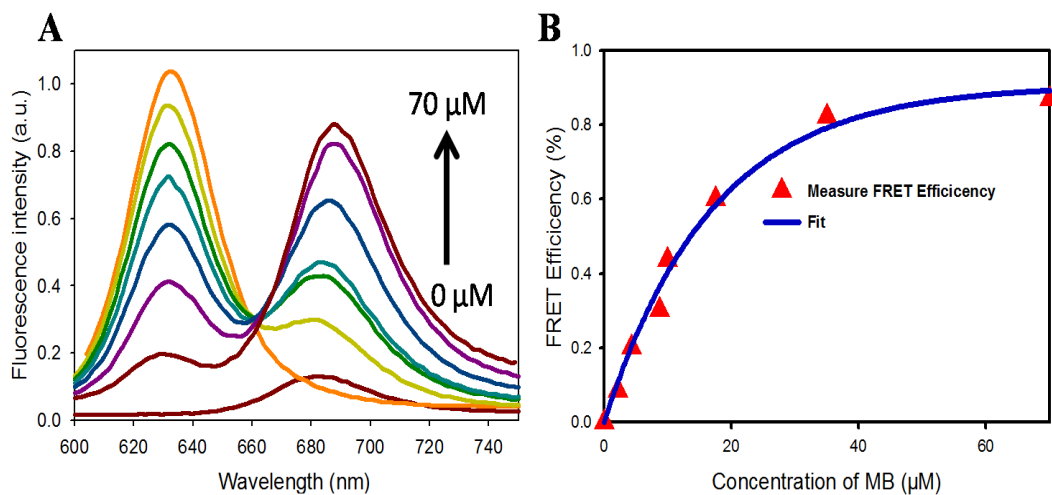


Figure S2. (A) FRET spectra of QDs/MB nanomicelles at different concentration of MB (from bottom to up: 0, 4.375, 8.75, 10.0, 17.5, 35.0, 70.0 μM), QDs concentration was at 85 nM; (B) Plot of FRET efficiency with different concentration of MB, derived from (A), and the fitting curve.

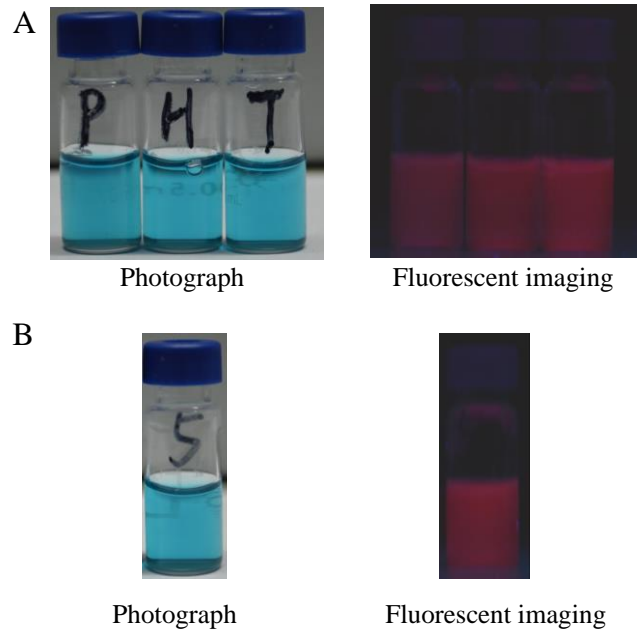


Figure S3. (A) Photograph and fluorescent imaging of QDs/MB nanomicelles dispersed at different buffer solutions, the buffers were PBS, HEPES and Tris-HCl at 10 mM, pH 7.4, from left to right, respectively. (B) Photograph and fluorescent imaging of QDs/MB nanomicelles after storing for 5 days.

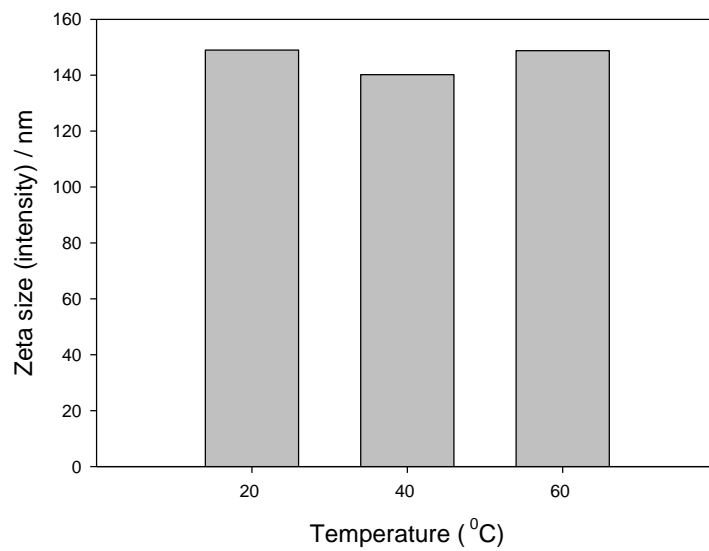


Figure S4. The thermal stability of the QDs/MB nanomicelles at different temperatures.

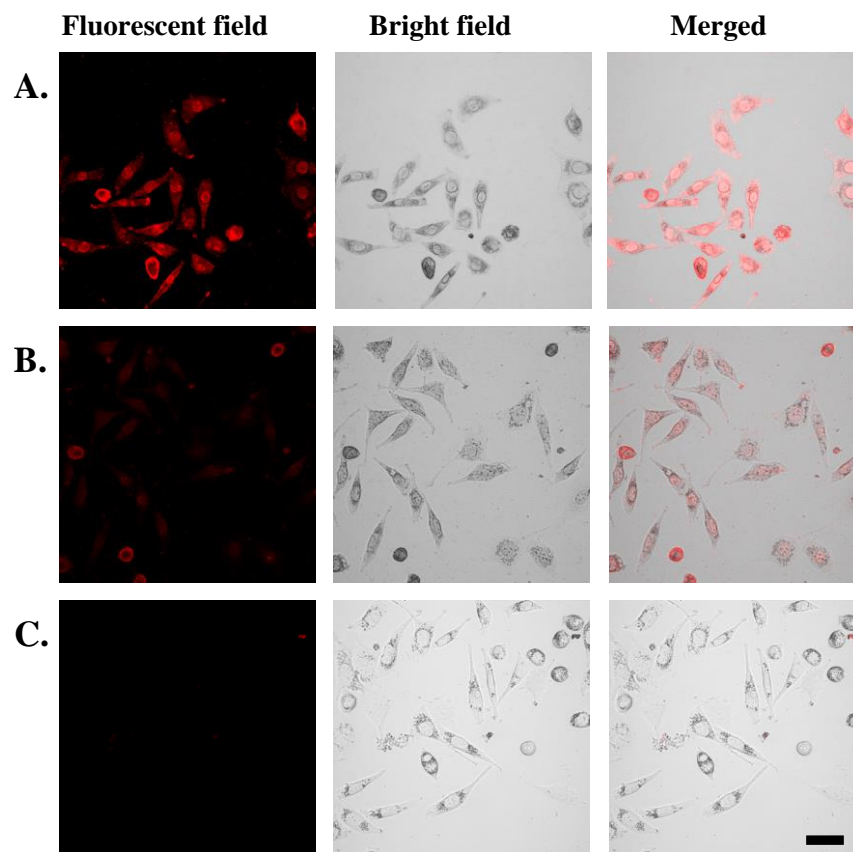


Figure S5. Laser scanning confocal microscopy image of liver cancer HepG2 cells incubated with QDs/MB nanomicelles (A), QDs nanomicelles (B) and MB nanomicelles (C) at 37 °C. (Excitation, 488 nm; emission 660 nm long-pass filter). Bar: 10 μ m.

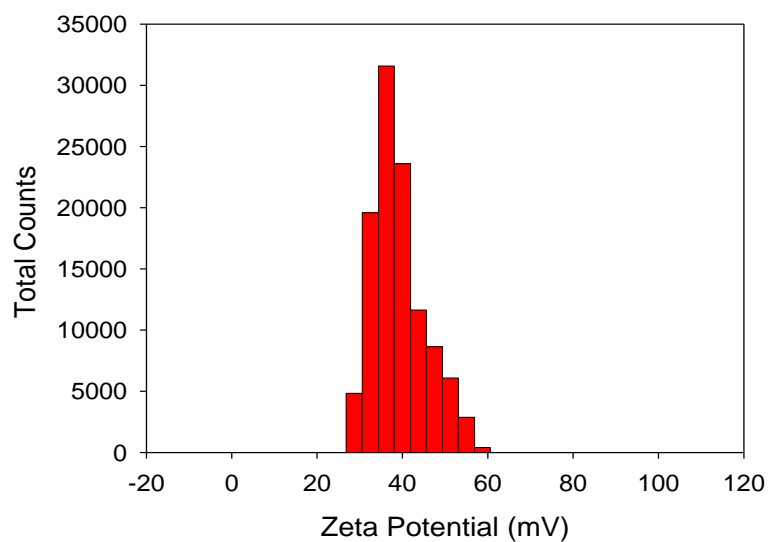


Figure S6. The zeta potential of the QDs/MB nanomicelles at pH 7.4.

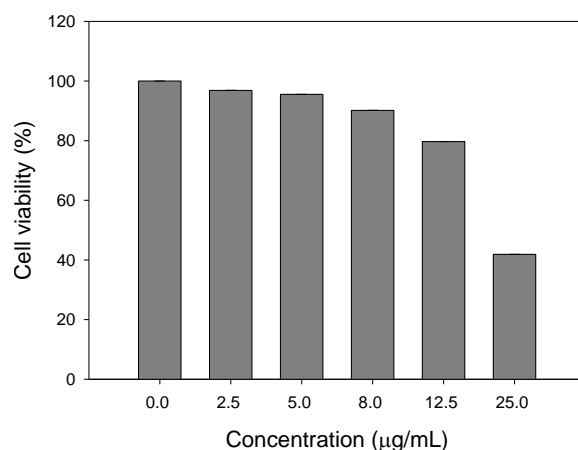


Figure S7. MTT experiment. Viability of HepG2 cells after being treated with different concentration of QD/MB nanomicelles for 24 h.

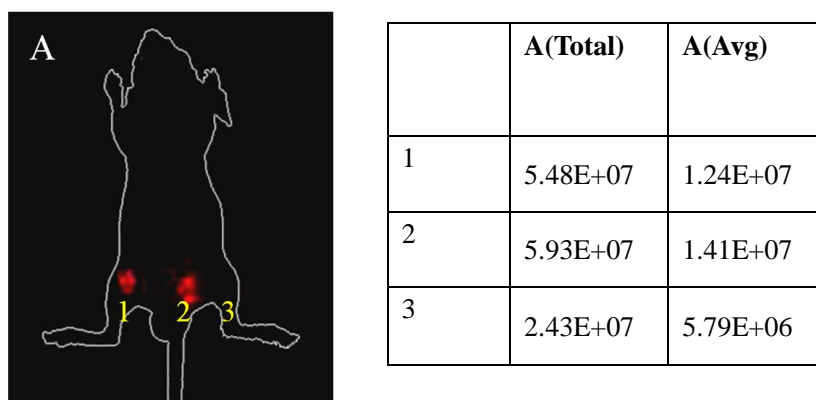


Figure S8. Fluorescence vivo images after subcutaneous injecting with different nanomicelles. (1) QDs nanomicelles, (2) QDs/MB nanomicelles, and (3) MB nanomicelles. The total and avg fluorescence intensity were calculated by the software of IVIS Lumina II in vivo imaging system. The total intensity means the integrated intensities in the region of interests. The avg intensity means the average intensities in the region of interests.

References

- 1 J. J. Li, Y. A. Wang, W. Guo, J. C. Keay, T. D. Mishima, M. B. Johnson and X. Peng, *Journal of the American Chemical Society*, 2003, **125**, 12567.
- 2 J. Liu, X. Yang, K. Wang, Y. He, P. Zhang, H. Ji, L. Jian and W. Liu, *Langmuir*, 2012, **28**, 10602.
- 3 J. Lakowicz, in *Principles of Fluorescence Spectroscopy*, Springer US, 2006, pp. 443-475.
- 4 J. Geng, Z. Zhu, W. Qin, L. Ma, Y. Hu, G. G. Gurzadyan, B. Z. Tang and B. Liu, *Nanoscale*, 2014, **6**, 939.
- 5 G. A. Crosby and J. N. Demas, *The Journal of Physical Chemistry*, 1971, **75**, 991.